Using gravitational wave parallax to measure the Hubble parameter with pulsar timing arrays

Daniel J. D'Orazio[*]

Department of Astronomy, Harvard University, 60 Garden Street Cambridge, Massachusetts 01238, USA
and Niels Bohr International Academy, Niels Bohr Institute, Blegdamsvej 17, 2100 Copenhagen, Denmark

Abraham Loeb

Department of Astronomy, Harvard University, 60 Garden Street Cambridge, Massachusetts 01238, USA

We demonstrate how pulsar timing arrays (PTAs) yield a purely gravitational wave (GW) measurement of the luminosity distance and comoving distance to a supermassive black hole binary source, hence providing an estimate of the source redshift and the Hubble constant. The luminosity distance is derived through standard measurement of the chirp mass, which for the slowly evolving binary sources in the PTA band can be found by comparing the frequency of GW-timing residuals at the Earth compared to those at distant pulsars in the array. The comoving distance can be measured from GW-timing parallax caused by the curvature of the GW wave fronts. This can be detected for single sources at the high-frequency end of the PTA band at distances up to 10 Gpcs with a future PTA containing well-timed pulsars out to $\mathcal{O}(10)$ kpc, when the pulsar distance is constrained to less than a GW wavelength. While, for the farthest pulsars, achieving this precision in pulsar distance measurements poses a great challenge, it may be met by future spaced-based very long baseline interferometry (VLBI) pulsar distance measurements coupled with GW-based pulsar distance measurements. Such a future PTA, with $\gtrsim 30$ pulsars with precise distance measurements between 1 and 20 kpc, could measure the Hubble constant to better than 30% for a single source at $0.1 \lesssim z \lesssim 1.5$. At $z \lesssim 0.1$, the luminosity and comoving distances are too similar to disentangle, unless the fractional error in the luminosity distance measurement is decreased below 10%. At $z \gtrsim 1.5$, this measurement will likely be restricted by a signal-to-noise ratio threshold. Generally, clarification of the different types of cosmological distances that can be probed by PTAs, and their relation to pulsar distance measurements is important for ongoing PTA experiments aimed at detecting and characterizing GWs.

I. INTRODUCTION

Gravitational waves (GWs) from coalescing compact object binaries are now being used to measure cosmological parameters. This new handle on cosmology is an important tool for understanding systematics in our current measurements of the cosmological parameters, e.g., for resolving the existing tension between different measures of the Hubble constant [1–3].

Direct measurements of the Hubble constant rely on knowledge of the redshift of an emitting source in addition to a determination of its intrinsic luminosity, be it GW or electromagnetic (EM), which is used to determine the luminosity distance. Comparison of the redshift and distance yields the Hubble constant. For example, the backbone of the standard candle approach [2] leverages the Leavitt Law [4] to relate the oscillation period of Cepheid variable light curves to the intrinsic luminosity, while a redshift is measured from the frequency shift of spectral lines in the host galaxy. The standard sirens approach [5–10] uses the predicted GW strain and frequency evolution of a coalescing binary to determine a luminosity distance, while again relying on an EM determination of the redshift, z.

While both are vital techniques, contributing independent measures of cosmology, the former relies on theoretical knowledge of standard candles and their astrophysical environments, e.g., supernovae, [11] while the latter relies on the existence of an EM counterpart that can be identified with the GW source, and hence understanding EM emission mechanisms. Additionally, both approaches only apply out to distances where EM emission can be detected.

The few methods that have been proposed to make cosmological measurements with GWs alone make use of inferred knowledge of the rest-frame GW source properties. For example, [12,13] rely on models of the rest frame neutron star mass distribution to break the mass-redshift degeneracy of inspiraling neutron star binaries. This is required because of the scale invariance of the binary

[*]djdorazio@gmail.com

merger problem. The GW luminosity is independent of the binary mass (which is why a luminosity distance can be measured), and the quantity $\mathcal{M}f$, the chirp mass times the GW frequency, is invariant with redshift. Hence, one must obtain knowledge about intrinsic source properties to make a joint redshift and luminosity distance determination, or one must introduce a new scale to the problem.

Here we do the latter. We propose a method for probing the distance-redshift relationship, and hence, measure the Hubble constant, via gravity alone, and without making assumptions about the GW source. While we cannot break the scale invariance of the binary merger problem, we can infer the redshift through a different means, with a large detector whose components are separated widely enough to detect the GW wave front curvature. Measurement of this curvature through the timing parallax will provide a distance to the source that is formally a comoving distance. The co-moving distance, D_c, is related to the luminosity distance, D_L, through $D_c = (1+z)^{-1}D_L$. A separate determination of the luminosity distance from the GW chirp and amplitude gives the redshift. Comparison of redshift and luminosity distance yields the Hubble constant up to choices of the cosmological density parameters.

Such a determination of the comoving distance from GW wave front curvature is not possible with current interferometric GW detectors such as LIGO [14] and LISA [15], which are sensitive to GWs from compact-object binary mergers ranging in mass from a few to $\sim 10^7 \, M_\odot$. However, Ref. [16] (hereafter DF11) shows that it is possible with the galaxy-scale pulsar timing arrays [PTAs, [17]], which are expected to detect low frequency GWs from the biggest black hole mergers in the Universe with masses of 10^8–$10^{10} \, M_\odot$, within the next decade [18]. We rederive this result with the important clarification that the distance recovered in this manner is indeed a comoving distance, not a luminosity distance as posited in DF11.

II. DISTANCE MEASUREMENTS WITH PTAs

The PTAs employ millisecond pulsars (MSPs) across the galaxy as precise clocks. A GW passing through the Earth-pulsar array will cause detectable deviations in the arrival times of the otherwise steady pulses that, when meticulously separated from non-GW induced timing residuals due to intrinsic changes in pulsar period and the intervening Earth-pulsar medium [19], will allow the detection of GWs in the 1–100 nHz frequency band. This is the relevant band for tracking the late inspiral of the most massive, 10^8–$10^{10} \, M_\odot$ black holes binaries at the hearts of massive galaxies [20].

Unlike their high-frequency interferometric-detector cousins, LIGO and LISA, one of the PTA's primary targets is a stochastic background of GWs, an astrophysical noise floor generated by the superposition of many inspiraling supermassive black hole binaries across cosmic distance [21,22]. Above this noise floor, it is expected that a number

of single resolved binary sources will also be detected, where different population models place this number at $\mathcal{O}(1$–$10)$ for near future arrays [18,23–25]. Here, we focus on the single resolved binary sources and show how a luminosity distance and a comoving distance can be measured for a subset of them.

A. Luminosity distance

It is well known that the luminosity distance can be measured for binary GW sources when their frequency evolution can be detected (e.g., [5,9]). So-called chirping binaries allow measurement of the chirp mass $\mathcal{M}$ and the GW strain h. In the source frame these are related by

$$h \propto \frac{\mathcal{M}_s^{5/3} f_s^{2/3}}{D_c}, \qquad (1)$$

where s denotes the source frame and D_c is the comoving distance. Because the strain h and GW frequency f can be measured over time, and the chirp mass can be measured from the first time derivative of the frequency (or the chirp, see [7,26]), Eq. (1) allows a measurement of the distance. In the observer's frame, the redshift of the frequency and its derivative implies that the strain, written in terms of observables, reads

$$h \propto \frac{\mathcal{M}_o^{5/3} f_o^{2/3}}{D_L}, \qquad (2)$$

where o denotes the observer's frame and the measurable distance is $D_L = (1+z)D_c$, the luminosity distance.

Whether or not a binary is chirping in the detectable band is set by the timescale for GW frequency evolution. For a binary on a circular orbit,

$$t_{\text{chirp}} \sim \frac{f}{\dot{f}} = \frac{5}{96} \left(\frac{G\mathcal{M}}{c^3}\right)^{-5/3} (\pi f)^{-8/3}$$
$$\approx 5.43 \times 10^3 \, \text{yr} \left(\frac{\mathcal{M}}{10^9 \, M_\odot}\right)^{-5/3} \left(\frac{f}{\text{yr}^{-1}}\right)^{-8/3}. \qquad (3)$$

For the high frequency and low mass binary inspirals and mergers detected by LIGO ($M = 1$–$10^3 M_\odot$, $f = 10$–10^4 Hz), and in the future, by LISA ($M = 10^2$–$10^7 \, M_\odot$, $f = 10^{-4}$–10^{-1} Hz), t_{chirp} is short compared to observation times and determination of the chirp mass and luminosity distance is expected. For the PTAs, however, Eq. (3) shows that the time for the GW frequency to evolve in the PTA band can be thousands of years. Hence, it is often assumed that only the combination $\mathcal{M}_o^{5/3}/D_L$ is measurable for binary GW sources in the PTA band.

However, a number of works discussed below have pointed out that chirp information in the PTA band can be gleaned by incorporating the many thousand year light travel time across the Earth-pulsar detector. Because the

timing residuals measured on Earth are a culmination of the entire path traveled by a EM pulse between the pulsar and Earth, the chirp can be detected by comparing the GW signal at the pulsar (pulsar term) compared to the signal at Earth (Earth term). Chirp detection then requires that the change in GW frequency at the detector (Earth-pulsar system), over the course of the light travel time across the detector, be larger than the frequency resolution of the detector. Conservatively, the frequency resolution is given by the inverse of the observation time, $\Delta f = 1/t_{\rm obs}$, e.g., [27,28]. Hence the condition on the Earth-pulsar distance L needed to measure the GW chirp is

$$L \geq \frac{c}{\dot{f} t_{\rm obs}} \approx 0.08 \,{\rm kpc} \left(\frac{\mathcal{M}}{10^9 \, M_\odot}\right)^{-5/3} \left(\frac{f}{\rm yr^{-1}}\right)^{-11/3} \left(\frac{t_{\rm obs}}{20\,{\rm yr}}\right)^{-1}. \tag{4}$$

For standard pulsar distances in present day PTAs of 0.1–1 kpc, this condition is met for the high frequency, high mass end of the expected binary population detectable by the PTAs. Longer pulsar baselines of future arrays, reaching out to 20 kpc (see Sec. III A), could allow chirp detection from the largest, $10^{10} \, M_\odot$, binaries down to a few tens of nHz, or from the smaller, $10^8 \, M_\odot$, binaries at ∼100 nHz.

The parameter space of binaries that meet this criterion and have a detectable strain is explored further in Ref. [29], while Ref. [30] discusses the region of binary parameter space where assuming zero-frequency evolution could be detrimental for detection. Reference [27] uses the synthetic population of supermassive black hole binaries from Ref. [23] and shows that the majority will have resolvable chirps when taking into account the pulsar term. While both studies point this out, the primary focus of these works is not binary frequency evolution, and so the chirp was ignored. Reference [31], however, investigates recovery of the luminosity distance with PTAs from such pulsar-term, chirping binaries. They assume an SNR = 20 detection, with 20 pulsars each having a 100 ns timing residual and randomly oriented on the sky at distances between 0.5–1 kpc. They find that the fractional error on the distance can be as low as 7% for edge-on inclination binaries ($i = \pi/2$) and rises to 30% for $i = \pi/4$. We take the findings from the above studies as conservative estimates of how well the luminosity distance can be recovered as they each assume pulsar distances on the order of 1 kpc, where, as discussed in the next section, we are interested in more futuristic PTAs that contain well-timed pulsars out to 20 kpc.

B. Comoving distance

We now show for the first time how PTA observations of GWs from a resolved, single-binary source can independently measure the source comoving distance.

1. Geometrical argument

The amount by which the arrival time of the EM pulses to Earth deviates due to a passing GW is dependent upon the changing amplitude, frequency, and phase of the GW encountered by the EM pulse at it traverses the Earth-pulsar distance. This is dependent on the shape of GW wave fronts, surfaces of constant GW phase, across the Earth-pulsar system. For very distant GW sources, the GW wave fronts can be assumed to be planar. However, for nearby sources, the true spherical nature of the wave fronts becomes non-negligible and encodes the source distance.

Figure 1(a) illustrates a geometrical argument that elucidates this concept and provides an estimate of when wave front curvature is important. Our setup consists of the detector: Earth and a pulsar separated by a distance L aligned at an angle θ relative to the line of sight of a source of GWs with observed frequency f at comoving distance D_c.

Without loss of generality, we consider the case where, under the plane wave approximation, GWs emitted at some time in the source frame arrive at the Earth and the pulsar after the same travel time. For spherical wave fronts, the travel time to the pulsar differs by $\delta t = \delta x / c$ [Fig. 1(a)], causing an EM pulse to traverse a different accumulated GW phase along its path. In comoving (flat-space) coordinates, we can compute δt via Euclidean geometry,

$$\delta t = \frac{D_c}{c} \left[\sqrt{1 + \left(\frac{L}{D_c}\right)^2} - 1 \right] \approx \frac{1}{2} \left(\frac{L}{D_c}\right) \frac{L}{c}. \tag{5}$$

This extra travel time compared to the plane wave case only affects the pulse arrival time if the EM pulse encounters a significant extra portion of a GW cycle. Hence, a condition
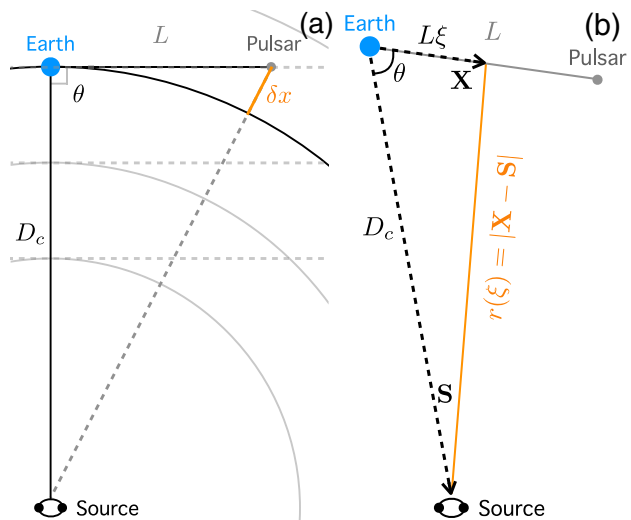

FIG. 1. Schematics for visualizing the geometrical (a), Sec. II B 1, and mathematical (b), Sec. II B 2, description of the comoving distance measurement. In (a), we assume $\theta = 90°$ to simplify the geometrical argument.

on there being a significant difference between timing residuals in the plane wave and spherical-wave cases is found from requiring that $\delta t f \gtrsim 1$ (noting that at exact integer values there is no change). This places a limit on the distances D_c and L for which wave front curvature is important,

$$D_c \lesssim f \frac{L^2}{c} = \left(\frac{L}{\lambda}\right) L, \qquad (6)$$

where $\lambda = c/f$, in analogy to the Fresnel condition in optics.

Because our observable is influenced by the relative time of arrival of GW wave fronts across the Earth-pulsar system, the distance to the source, D_c, must be a comoving distance that takes into account time dilation along the path of GWs from the source at an earlier time in the Universe,

$$D_c = c \int_{t_{\text{src}}}^{t_0} \frac{dt}{a(t)}, \qquad (7)$$

where $a(t)$ is the scale factor of the expanding universe at time t, t_0 denotes the observation time, and t_{src} denotes the emission time at the source. Because f and L are present-day observed quantities in Eq. (6), it is the comoving distance that is encoded in the pulsar timing residuals measured at Earth. Another way to see this is to recognize that the GW phase, Φ, is the relevant quantity governing the timing residual, and the GW phase, $\Phi \propto \int f(1+z) dt$, where $f(1+z)$ is the GW frequency at redshift z along the path. Since $a(t) = (1+z)^{-1}$, then $\Phi \propto \int \frac{dt}{a(t)} \propto D_c$.

2. Mathematical argument

Following DF11, we outline the derivation of the pulse arrival time correction due to curved GW wave fronts. Building upon our previous setup, we illustrate relevant quantities for the derivation in Fig. 1(b).

Assuming that the pulsar emits regular pulses at a much higher frequency than that of the passing GW (however, see [32]), the extra light travel time of a given pulse due to the passing GW, the arrival time correction, is given by [33–35]

$$t_{\mathcal{GW}}(t) = \frac{1}{2} \hat{n}^i \hat{n}^j \mathcal{H}_{ij}, \qquad (8)$$

$$\mathcal{H}_{ij} = \frac{L}{c} \int_{-1}^{0} h_{ij} \left[t + \frac{L}{c} \xi, -L\xi\hat{n} \right] d\xi, \qquad (9)$$

which is the integral of each component of the transverse-traceless GW metric perturbation $h_{ij}(t, \mathbf{x})$ along a null geodesic connecting the pulsar and the Earth, parametrized

by ξ.[1] Here $\mathbf{P}$ is the position of the pulsar and $\hat{\mathbf{n}}$ is the unit vector pointing from Earth to the pulsar.

Writing out the strain as a function of the spacetime coordinates in the source frame, and in terms of the Fourier components,

$$
\begin{aligned}
&h_{ij}(t, \mathbf{X}) \\
&= \frac{1}{|\mathbf{X} - \mathbf{S}|} \int_{-\infty}^{\infty} [\tilde{A}_{ij}(f_s, \hat{\mathbf{k}}) e^{2\pi i f_s |\mathbf{X} - \mathbf{S}|/c}] e^{-2\pi i f_s t} df_s d^3 k,
\end{aligned}
\qquad (10)
$$

where the s subscript labels the source frame with no red-shifting of the frequency. Here $\mathbf{X}$ is the vector pointing from Earth to the EM pulse wave front that is traveling the null geodesic connecting the Earth and pulsar, $\mathbf{X} = L\xi\hat{\mathbf{n}}$. $\mathbf{S}$ is the vector pointing from the Earth to the source, $\mathbf{S} = D_c\hat{\mathbf{s}}$, where D_c is the comoving distance to the source. The quantities $\tilde{A}_{ij}$ are the components of the wave strength.

The spherical GW wave front propagates along the unit vector,

$$\hat{\mathbf{k}} = \frac{\mathbf{X} - \mathbf{S}}{|\mathbf{X} - \mathbf{S}|}. \qquad (11)$$

The magnitude $|\mathbf{X} - \mathbf{S}|$, namely the distance from source to wave front at point $\mathbf{X}(\xi)$, can be found by the law of cosines. For a flat universe in comoving coordinates,

$$r(\xi) \equiv |\mathbf{X} - \mathbf{S}| = D_c \left[1 + \left(\frac{L\xi}{D_c}\right)^2 + 2\frac{L\xi}{D_c} \cos\theta \right]^{1/2}. \qquad (12)$$

Note that the GW amplitude is proportional to $\tilde{A}_{ij}/r(\xi)$, which reduces to $\tilde{A}_{ij}/D_c$, as expected for $D_c \gg L$.

Combining Eqs. (8)–(12), keeping terms to $\mathcal{O}(L/D_c)$, integrating, and separating terms in order of L/D_c, we find the expression for the plane wave and first-order-curvature pulse travel-time corrections in Fourier space, matching Eq. (10) of DF11. To write their expression in a more elucidating form, we define

$$
\begin{aligned}
\Delta T &\equiv \frac{[\hat{n}^i \hat{n}^j \tilde{A}_{ij}]_s}{2\pi f_o D_c} e^{2\pi i f_s D_c/c} \\
&\propto \frac{\mathcal{M}_s^{5/3} f_s^{2/3}}{2\pi f_o D_c} e^{2\pi i f_s D_c/c} \mathcal{Q}(\alpha_P, \beta_P, \phi, \phi_0, I, \psi),
\end{aligned}
\qquad (13)
$$

where in the last line we write out the $\tilde{A}_{ij}$ dependence assuming circular binary orbits. The function $\mathcal{Q}$ depends on

---

[1]Note that for our purposes it is sufficient to compute this pulse travel-time correction due to the intervening GW. Whereas the "timing residual" often encountered in the literature (e.g., [36]), is this quantity divided by the pulsar period and integrated over the observation time.

the pulsar position angles (α_P, β_P), the binary orbital phase ϕ and phase reference ϕ_0, the binary inclination I, and the polarization angle ψ. The other two angles of importance, the angular position of the GW source (α, β), appear outside of ΔT through the angle θ,

$$\cos\theta = \cos\beta\cos\beta_P\cos(\alpha - \alpha_P) + \sin\beta\sin\beta_P. \quad (14)$$

Importantly, the denominator of Eq. (13) includes the frequency at the Earth-pulsar detector. This is because the observed timing residual is set by the observed strain over the observed GW frequency. To put the above into observed quantities for sources at cosmological distance, use that $\mathcal{M}_o = (1+z)\mathcal{M}_s$ and $f_o = (1+z)^{-1}f_s$. Therefore,

$$\frac{\Delta T_o}{\mathcal{Q}(\alpha_P, \beta_P, \phi, \phi_0, I, \psi)} \propto \frac{\mathcal{M}_o^{5/3}f_o^{-1/3}}{2\pi D_L}e^{2\pi i f_0 D_L/c}, \quad (15)$$

where the luminosity distance $D_L = (1+z)D_c$.

Using our definition of ΔT_o, the Fourier travel-time correction, broken into plane wave and first-order curvature parts, becomes

$$\tau_{\mathcal{GW}} = \tau_{\text{pw}} + \tau_{\text{cr}}$$
$$= \frac{\Delta T_o}{2}\left\{\exp\left(2\pi i\frac{f_o L}{c}\sin^2\frac{\theta}{2}\right)\frac{\sin\left(2\pi\frac{f_o L}{c}\sin^2\frac{\theta}{2}\right)}{\sin^2\frac{\theta}{2}}\right.$$
$$\left. + 2(1+\cos\theta)\exp\left[\pi i\frac{f_o L}{c}\left(4\sin^2\frac{\theta}{2} + \frac{L}{2D_c}\sin^2\theta\right)\right]\frac{\sin\left(\frac{\pi f_o L^2}{2cD_c}\sin^2\theta\right)}{\sin^2\theta}\right\}. \quad (16)$$

Both terms still have a dependence on the distance through the usual $1/D_L$ in ΔT_o. However, the curvature term now has a dependence on $f_o L^2/D_c$. Because we can independently measure f_o and L, this term introduces a way to measure the comoving distance separately from the luminosity distance.

The form of the travel-time correction also confirms our simple geometric argument of the previous subsection, that the curvature term decreases in importance as $\pi f_o L^2/(2cD_c)\sin^2\theta \to 0$. Indeed when $D_c \gg \frac{f_o L^2}{c}$, the wave front curvature can be neglected. For values expected for near-future PTAs, the timing residual due to the wave front curvature corrections will be of order the plane wave residual when

$$\frac{\pi f_o L^2}{2cD_c} = 0.5\left(\frac{f_o}{\text{yr}^{-1}}\right)\left(\frac{L}{10\text{ kpc}}\right)^2\left(\frac{D_c}{1\text{ Gpc}}\right)^{-1}. \quad (17)$$

Note that the dependence on pulsar distance is approximately quadratic for $\sin(\pi f_0 L^2/(2cD_c)) \sim \pi f_0 L^2/(2cD_c)$, which is valid up to $L \sim 10$ kpc in the above example. Hence, if future PTAs can precisely time pulsars out to 10–20 kpc, then the comoving distance can be probed through GW-timing parallax, at the same sensitivity as required for detection of the plane wave terms, out to Gpcs—for all conceivable supermassive black hole binary mergers detectable by PTAs. If the GW detection has a high signal-to-noise ratio (SNR), then even greater distances can be probed. However, in addition to the criteria considered thus far, measurement of the wave front curvature also requires a precise measurement of the pulsar distance, which we discuss below.

III. HUBBLE CONSTANT MEASUREMENT

When both the luminosity distance and the comoving distance can be measured, and distinguished from each other, for the same binary GW source, the redshift and hence Hubble constant H_0 can be measured. To distinguish the two distances we require that the fractional errors on D_L and D_c be less than $(D_L - D_c)/D_c = z$, which is ~ 0.25 at 1 Gpc. When this is possible, the redshift of the source can be recovered with uncertainty,

$$\delta z = \sqrt{\left(\frac{\delta D_L}{D_c}\right)^2 + \left(\frac{D_L}{D_c}\frac{\delta D_c}{D_c}\right)^2} \quad (18)$$

and can be used to measure the Hubble constant via

$$H_0 = \frac{c}{D_c(z)}\int_0^z\frac{dz'}{E(z')}, \quad (19)$$

with relative uncertainty,

$$\frac{\delta H_0}{H_0} = \sqrt{\left(\frac{\delta z}{E(z)}\right)^2\left(\int_0^z\frac{dz'}{E(z')}\right)^{-2} + \left(\frac{\delta D_c}{D_c}\right)^2}. \quad (20)$$

A. Distance measurement precision and PTA dependence

We estimate the fractional error in the Hubble constant measurement by considering PTA detections above a cutoff SNR and hence a constant fractional error on D_L. As a fiducial value we use $\delta D_L/L \sim 10\%$ estimated in [31] for

detections with a SNR of 20 (see Sec. II A). Next, we numerically estimate the precision in the $D_c(z)$ measurement.

B. Main challenges

A requirement for the measurement of D_c is that the pulsar coordinates are precisely known, to within approximately a GW wavelength. While this does not impose a stringent constraint on the measured precision of the pulsar angular coordinates, it does strongly constrain the required precision on the pulsar distance measurement (e.g., DF11, [31]).

This δL requirement is seen geometrically from Fig. 1(a). Imagine that the pulsar is at distance L and angle $\theta = \pi/2$. In the plane wave limit the GW phase observed at Earth is $\Phi = \Phi_0 + 2\pi f(t - L/c)$, while for spherical wave fronts the phase is approximately $\Phi = \Phi_0 + 2\pi f[t - L/c(1 - L/D_c)]$. Hence, if L is not known to within $\delta L \lesssim (L/D_c)L$, which is approximately $\lambda_{\mathcal{GW}}$ in the limit of Eq. (6), one cannot distinguish between a phase difference due to a different L or due to the L/D_c correction. In Fig. 1 this translates to moving the pulsar to a different distance in the plane wave approximation or keeping it fixed but with differently curved wave fronts (different D_c).

One might expect a similar requirement exists for D_L, as it also relies on including combined phase information at the pulsar and at Earth. However, this requirement can be circumvented by simultaneously fitting for the pulsar distances in a joint analysis with the binary properties and D_L. The timing residual from each pulsar is modulated at the beat frequency between the GWs at the Earth and at the pulsar, which encodes the chirp from which D_L is measured. As long as a residual is monitored for long enough to measure a beat modulation [the criteria of Eq. (4)], the chirp can be measured from $\dot{f} \propto c f_{\text{beat},i}/L_i$, for the ith pulsar. Hence simultaneous fitting for the L_i will yield the one value of $\dot{f}$, and so D_L, to higher precision with more pulsars. See also the discussion in [31,37].

We first demonstrate how the H_0 measurement depends on pulsar distance uncertainties and the number of pulsars in the array, we then turn to a discussion of the practicality of such measurements and suggestions for near-term work that should be done towards making such measurements a reality.

C. PTA dependence

We envision an idealized PTA with N_p pulsars having randomly drawn angular coordinates (α_i, β_i) on the sky, at randomly drawn distances L_i in the range $L_{\min}$ to $L_{\max}$, and with fractional distance errors measured in units of the gravitational wavelength $\lambda_{\mathcal{GW}}$, $\delta L/L = \chi \lambda_{\mathcal{GW}}/L_{\max}$. We consider further that, for each pulsar, the timing residual divided by the prefactor ΔT_o in Eq. (16) can be measured to

within a constant fractional error of $\delta\tau/\tau$. This essentially subsumes errors on the remaining binary parameters into $\delta\tau_i$ and will generally be dependent on the SNR.

We generate mock observed timing residuals by calculating the expected travel time correction, τ_i, from Eq. (16). We draw observed values $\tau_{\text{obs},i}$ from a normal distribution with mean and standard deviation given by τ_i and $\delta\tau_i$, respectively. We also draw observed pulsar distances $L_{\text{obs},i}$ from a normal distribution with mean and standard deviation given by L_i and δL_i, respectively. We recover the source parameters from the observed arrival time deviations by minimizing a least squares statistic that compares to the model, Eq. (16), but with $L_{\text{obs},i}$ as the input pulsar distances,

$$\sum_{i=1}^{i=N_p} (|\tau_{\mathcal{GW}}(D_c, \alpha, \beta, L_{\text{obs},i})| - |\tau_{\text{obs},i}|)^2, \qquad (21)$$

where $|\cdot|$ denotes the norm of the complex Fourier timing deviations. We impose a log-uniform prior on $\log D_c/\text{Mpc} \in [0, 5]$ and uniform priors on the angular source coordinates $\alpha \in [0, 2\pi], \beta \in [0, \pi]$. For fixed $\tau_{\text{obs},i}$, we carry out 100 such minimizations for 100 different realizations of the $L_{\text{obs},i}$. We quote the mean and standard deviation of the 100 sets of resulting source parameters as estimates for the recovered parameters and their uncertainties.

Throughout, we consider a fiducial PTA with N_p pulsars in the $L_{\min} = 1$ kpc to $L_{\max} = 20$ kpc distance range and a error on L parametrized in units of GW wavelengths. The fractional error on τ will be SNR dependent; for the purpose of this study, we choose a fiducial value of 10%. We study the affect of varying these choices below.

For computational purposes, we draw pulsar sky locations within $\pi/4$ from the optimal $\theta = \pi/2$. This means that an isotropic pulsar distribution would require twice the number quoted here, though, for a favorably positioned source, a pulsar distribution biased by the Milky Way plane would require less pulsars than our N_p suggests. We find below that a factor of a few in our predicted pulsar numbers is not significant compared to other uncertainties and may not be a limiting issue given that hundreds to thousands of pulsars may make up future PTAs [38]. Finally, we consider a fiducial GW source frequency of $f_o = 10^{-7}$ Hz, where the GW parallax distance determination is most effective.

Figure 2 shows how well our fiducial PTA recovers the comoving distance (left), longitude (middle), and latitude (right) of our GW source when it is placed at a redshift of $z = 0.25$ with angular positions $(\alpha, \beta) = (\pi/4, \pi/4)$. The top row shows that indeed the discussed requirement on the pulsar distance is borne out in our numerical propagation of errors experiment. Only for $\delta L \lesssim 0.5\lambda_{\mathcal{GW}}$ is a constraint made on the source parameters. For a 32 pulsar array, D_c is
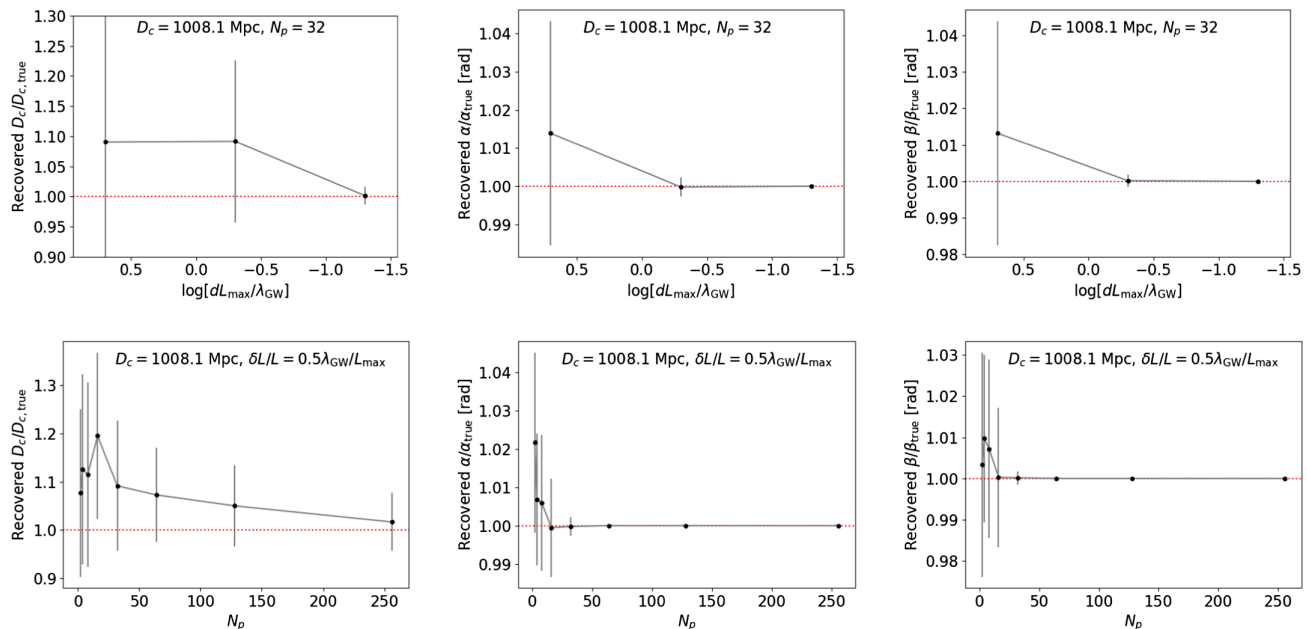
FIG. 2.   The recovered comoving distance, D_c, and sky coordinates (α, β) of the GW source for PTAs with varying numbers of pulsars and precision in the distance measurement of these pulsars. The considered PTAs assume pulsars lying between 1 and 20 kpc from Earth and with $\delta\tau/\tau = 0.1$. In the x-axis label of the top panel, dL_{max} refers to the worst precision in the array, on the most distant pulsars.

constrained at the 10% level for $\delta L/L = 0.5\lambda_{\mathcal{GW}}/L_{max}$, while the angular coordinates of the source are constrained to the sub-1% level. These source constraints tighten proportionally to δL. In the bottom row, we vary the number of pulsars in the $\delta L/L = 0.5\lambda_{\mathcal{GW}}/L_{max}$ array. We find that the source coordinates are poorly constrained for $N_p \leq 16$, but accuracy and precision of parameter recovery increase with increasing pulsar number. Increasing the number of pulsars for a PTA with $\delta L \geq \lambda_{\mathcal{GW}}$ does not allow a better (or any) measurement of the source parameters.

D. Precision of redshift and Hubble constant measurement

In the left panel of Fig. 3, we plot recovered comoving distances as a function of redshift (orange) for fiducial PTA and source properties and using 256 pulsars. For reference, we also plot the corresponding luminosity distances with 10% fractional errors (blue). The dotted lines show the theoretical expectation for each distance measure.[2] Accurate determination of luminosity and comoving distances, and hence determination of the source redshift, is possible when recovered values are consistent with the theoretical values, and when the blue and orange error bars do not overlap.

The right panel of Fig. 3 uses the distance errors in the left panel and Eqs. (18)–(20) to display the fractional error in the redshift and the Hubble constant measurements for

the corresponding points in the left panel. For this specific GW source ($\alpha = \beta = \pi/4$, $f = 10^{-7}$ Hz) and PTA, we find that the redshift and Hubble constant can be determined to better than order unity for $z \gtrsim 0.1$ and to within 40% for $z \gtrsim 0.5$. At $z \leq 0.1$, D_c and D_L are indistinguishable from each other, but their measurement could still impose upper limits on z and H_0. Choice of smaller $\delta D_L/D_L = 0.01$ decreases the redshift at which a determination of H_0 could be made, bringing the low-z side of the curve in the right panel of Fig. 3 down to the level of the high-z values, allowing 30–40% fractional errors on H_0 and z for $z \lesssim 1.5$.

To further demonstrate the dependence on PTA properties, Fig. 4 replicates Fig. 3 but now for a more optimistic scenario where the pulsar distances can be measured to a five times higher precision of $\delta L/L = 0.1\lambda_{\mathcal{GW}}/L_{max}$, but including eight times fewer pulsars ($N_p = 32$). In this case, the minimum redshift required for order-unity-precision distance measurements remains at $z = 0.1$, but $\leq 20\%$ level measurements of the Hubble constant are possible for $z \geq 1$. We do not consider higher redshifts as such binary GW sources are likely not detectable beyond this range with Square-Kilometer-Array (SKA)-era PTAs [23], though futuristic arrays may extend beyond these redshifts. Fractional errors on H_0 and z would decrease further for higher frequency sources, a better measurement of D_L, or the inclusion of more well-measured pulsars.

E. Beyond the pulsar distance constraint

Up until now we have only shown the dependence of the H_0 measurement on the parameters of a hypothetical PTA. Such a hypothetical PTA, however, requires pulsar distance

---

[2]We use $\Omega_M = 0.3$, $\Omega_\Lambda = 0.7$, and $h = 0.7$ throughout.
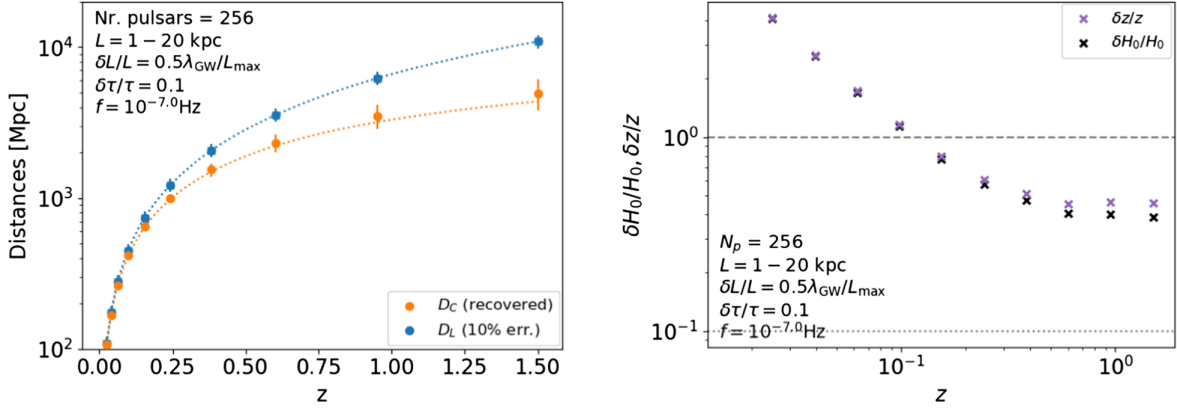
FIG. 3. Left: recovery of comoving and luminosity distances, D_c and D_L, vs redshift, z, for a PTA with 256 pulsars, with $\delta L/L = 0.5\lambda_{\mathcal{GW}}/L_{\max}$. Right: the corresponding fractional errors in the measured redshift and the Hubble constant. The fractional error in D_L is assumed constant.
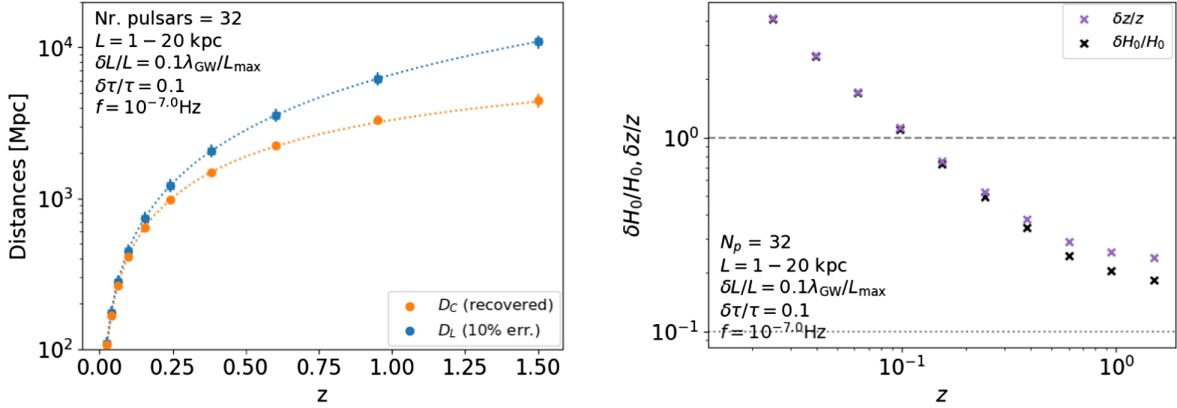

FIG. 4. Same as Fig. 3, but for 5× more precise pulsar distances but 8× fewer pulsars. Precise pulsar distances are clearly more important than the number of pulsars in the array.

uncertainties, $\delta L \lesssim \lambda_{\mathcal{GW}}$, which would pose a great challenge to achieve with present methods. This is because the GW wavelength of interest is $\lambda_{\mathcal{GW}} = 0.1$–$1.0$ pc for a $10^{-7.0}$–$10^{-8.0}$ Hz frequency range, which amounts to a precision on the pulsar distance that has been approached only for a few nearby pulsars (e.g., [39,40]). In the near future, precise pulsar distance measurements using parallax from VLBI determined astrometry will be able to achieve parallax angle uncertainties of $\delta p = \mu as$ resulting in $\delta L \sim \delta p/p^2$ distance measurements [41]. For $L = 1$ kpc, this is $\delta L \sim 1$ pc$(L/(1 \text{ kpc}))^2$. Hence, with astrometry limited to the μas level and without another way around the pulsar distance problem, the technique presented here would seem to be limited to using pulsars within 1 kpc, and so limits a comoving distance measurement to sources with $D_c \lesssim 100$ Mpc via Eq. (17).

One way beyond this is to look to space VLBI, where sub-μas astrometric limits are conceivable [42,43]. Though parallax uncertainties of $\sim 10^{-2}\mu as$ (sub-mm and higher

frequency VLBI over 10^6 km baselines) may be needed to achieve the required precision for pulsars out to 10–20 kpc.

In addition to relying on future high-precision pulsar distance determinations, it may be possible to use GW detections with near-future PTAs to measure the pulsar distances and build a ladder of precise distance measurements from the well measured nearby pulsars out to the distant pulsars, and then to the GW sources by means of GW parallax. We speculate on a few possible scenarios that could lead towards this goal:

(1) A calibrating GW source with known redshift could be used to measure the pulsar distances using the chirp and GW curvature for an entire array. The redshift could derive from localization of a host galaxy and/or an assumed cosmology coupled with a measured luminosity distance.

(2) A nearby source of GWs ($D_c \lesssim 100$ Mpc) could allow measurement of the comoving distance and source location using well-measured nearby pulsars

($L \leq 1$ kpc). The known source location could be used to update the coordinates of distant pulsars, which are more greatly affected by wave front curvature terms.

A rigorous analysis of these possibilities and, in general, the joint recovery of the luminosity, comoving, and pulsar distances is the subject of current and future work.

IV. DISCUSSION AND CONCLUSIONS

We have demonstrated that PTAs can measure both the luminosity distance and the comoving distance to a subset of resolved binary sources of GWs. In doing so, they can measure the source redshift and the Hubble constant. Thus the PTAs, by themselves, could become cosmological instruments. The distance out to which such a measurement can be made, however, depends on how well the distances to well-timed pulsars can be determined.

Currently, PTAs are operating with tens of pulsars at distances out to a few kpc. Distance errors range from a fraction of a percent to order unity, with some reaching down to the sub-pc level precision required to measure a comoving distance as described here (e.g., [39,40,44]). In the coming years, the SKA is expected to expand the pulsar population drastically [45]. Reference [38] estimates that ~6000 MSPs are detectable by the SKA out to $\mathcal{O}(10)$ kpc with better than 20% error on their distances. If ~5% of these are suitable for high precision timing (e.g., [46]) and also high precision distance measurements, either with future space-VLBI, or via GW-based pulsar distance measurements, then the PTAs envisioned here, with tens to hundreds of pulsars between 1 and 20 kpc and with $\lesssim$pc distance errors, could be realized. Note, however, that the most crucial MSPs are the most distant, and these may be the most difficult to time precisely due to a higher like-lihood for lower SNRs.

In constructing the mock PTAs of the previous section, we chose pulsars with a uniform distance distribution in order to study the dependence on pulsar number in a controlled way without dependence on a specific astro-physical spatial distribution. Our maximum pulsar distance in these calculation is consistent with the above quoted

MSP discovery simulations. However, these simulations do assume a galactic pulsar distribution informed by obser-vations. Hence, to see if the assumed pulsar spatial distribution affects our results, we rerun our N_p study but instead of drawing pulsar distances uniformly between L_{min} and L_{max}, we draw a pulsar galacto-centric radial distance from the distribution of Ref. [47] (Model C), and then randomly draw an azimuthal angle in the galactic disk to find the pulsar distance from Earth, which we situate at 8 kpc from the galactic center. The results are presented in Fig. 5, which is very similar to the bottom row of Fig. 2. Because it is the most distant pulsars that most strongly affect the D_C measurement, this agreement primarily tells us that a realistic galactic pulsar distribution, with no imposed limits on the pulsar distance, can provide the pulsars needed to make the measurement envisioned here. That such pulsars could be detected and timed in the SKA era is corroborated by the simulations carried out by, e.g., [38,46,48], though we have not included further possible selection effects related to difficulties in timing and measuring distances to the most distant pulsars. A more rigorous analysis of the application of near-future PTAs to this measurement is the focus of current work.

Note that Ref. [38] considers only galactic pulsars (see their Fig. 1); pulsars in the Magellanic clouds could provide MSPs out to 40–60 kpcs [49–52]. Though, again, without ultrahigh precision distance measurements, such distant pulsars may only be useful for measuring the luminosity distance, and not the comoving distance. In addition to the SKA, the next generation Very Large Array [53] and astrometric pulsar distance measurements with WFIRST [54] will make the pulsar-distance errors envisioned here even more feasible, at least for nearby $L \lesssim 1$ kpc pulsars. Such future arrays will also likely decrease the expected error in the luminosity distance measurement, and further reduce the error in the described Hubble constant measurement.

If the Hubble constant can be measured in this manner for tens of sources, then a PTA-only measured value could reach a few to 10% precision. While the number of such resolved "foreground" binaries that will be detected is uncertain and relies on the poorly constrained binary
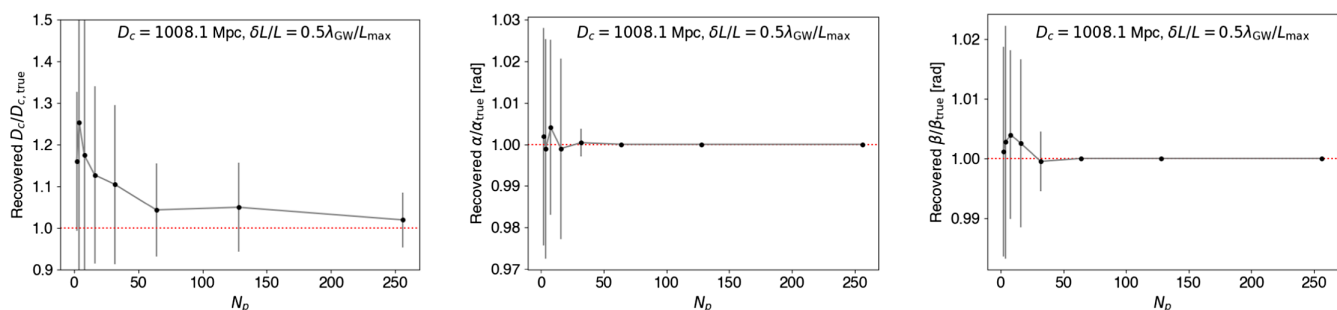

FIG. 5. The same as the bottom row of Fig. 2, but drawing the pulsar distances from the galacto-centric radial distribution of Ref. [47], with no constraints on the pulsar distribution.

population, multiple studies have attempted to estimate this number. Reference [18] estimates that it may indeed be the resolved single binary sources that are detected before a stochastic GW background, with a detection every few years. Older models suggest that the number of such detections may be an order of magnitude lower [23–25]. Reassuringly, Ref. [23] shows that the most probable redshift range for resolved sources is between $0.2 \lesssim z \lesssim 1.5$, in the right range for the measurement envisioned here. However, [18] shows that while the resolved single sources are the most common at the higher GW frequencies considered here $\sim 10^{-7}$ Hz, their amplitudes are lower and the PTAs are less sensitive at these frequencies. This leads Ref. [18] to conclude that the optimal single-source detection frequencies for near future PTAs lie at $\sim 10^{-8}$ Hz. At these lower frequencies, the GW parallax measurement is more difficult, as the curvature term is less important for a GW binary at the same distance [Eq. (17)], however, at lower frequencies the requirement on the pulsar distance uncertainty is lessened by the same amount. Future work could analyze expected supermassive black hole binary populations in light of the measurement at hand, quantifying how many sources per redshift and frequency will contribute to a meaningful measurement of the Hubble constant.

For nearby GW sources ($z \lesssim 0.1$), we found that only upper bounds on the redshift and Hubble constant can be set because D_c and D_L are within 10% of each other. This is partly due to our adopted 10% fractional error on the luminosity distance measurement. If this can be improved upon, as it very well could be by the time that the D_c measurement is feasible, then one can take advantage of more nearby sources. In addition, because the comoving distance can be measured to high precision for these nearby sources, its measurement could facilitate identification of the binary host galaxy (as discussed in DF11), and allow a standard-siren-type determination of the Hubble constant, as well as offer important astrophysical insight into, e.g., the morphology of supermassive black hole binary host galaxies.

While we have provided a proof-of-principle error estimation focusing on the largest error sources, future work should consider more realistic parameter estimation techniques, and the precision and accuracy to which all of the binary parameters can be recovered jointly (e.g., [55,56]).

For example, by not modeling the orbital geometry of the GW source, we do not include binary inclination or GW polarization factors that would affect the degree with which inclination and luminosity distance can be disentangled. Furthermore, we have not included the frequency evolution of the binary when including the wave front curvature terms in the arrival time corrections, but this will be necessary for joint recovery of the luminosity and comoving distances. Finally, techniques that independently fit for the pulsar distances as part of the model (e.g., [29,37]) could enhance the precision of source parameter recovery presented here and should also be considered for application to cosmology with PTAs.[3]

In summary, we have presented a novel method by which to measure the Hubble constant without the use of EM radiation, by assuming only general relativity, and without the need to model astrophysical properties of the emitting source of radiation. This measurement can be made uniquely by future PTAs that can determine the distances to well-timed pulsars to sub-pc precision. Depending on the distance to pulsars for which such a distance measurement can be made, this would result in a single-source determination of the Hubble constant at the tens of percent level out to redshifts of $z \lesssim 1.5$. Tens of such detections could yield a $\lesssim 10\%$ measurement of the Hubble constant from gravitational signals from cosmological sources.

---

[3]During the review process, [36] posted a preprint detailing recovery of binary GW source parameters including a distance using the curvature of GW wave fronts while including the changing GW frequency across the Earth-pulsar baseline. No work has yet differentiated the comoving and luminosity distances in such an analysis.

[1] A. G. Riess, L. M. Macri, S. L. Hoffmann, D. Scolnic, S. Casertano, A. V. Filippenko, B. E. Tucker, M. J. Reid, D. O. Jones, J. M. Silverman, R. Chornock, P. Challis, W. Yuan, P. J. Brown, and R. J. Foley, Astrophys. J. **826,** 56 (2016).

[2] A. G. Riess, S. Casertano, W. Yuan, L. M. Macri, and D. Scolnic, Astrophys. J. **876,** 85 (2019).

[3] P. A. R. Ade, N. Aghanim, M. Arnaud, M. Ashdown, J. Aumont, C. Baccigalupi, A. J. Banday, R. B. Barreiro,

J. G. Bartlett *et al.* (Planck Collaboration), Astron. Astrophys. **594,** A13 (2016).

[4] H. S. Leavitt and E. C. Pickering, Harvard College Observatory Circular **173,** 1 (1912), https://ui.adsabs.harvard.edu/abs/1912HarCi.173....1L.

[5] B. F. Schutz, Nature (London) **323,** 310 (1986).

[6] A. Krolak and B. F. Schutz, Gen. Relativ. Gravit. **19,** 1163 (1987).

[7] D. E. Holz and S. A. Hughes, Astrophys. J. **629,** 15 (2005).

[8] C. Cutler and D. E. Holz, Phys. Rev. D **80,** 104009 (2009).

[9] B. P. Abbott, R. Abbott, T. D. Abbott, F. Acernese, K. Ackley, C. Adams, T. Adams, P. Addesso, R. X. Adhikari, V. B. Adya *et al.*, Nature (London) **551,** 85 (2017).

[10] H.-Y. Chen, M. Fishbach, and D. E. Holz, Nature (London) **562,** 545 (2018).

[11] M. Rigault, V. Brinnel, and G. e. a. Aldering, Astron. Astrophys. **644,** A176 (2020).

[12] S. R. Taylor and J. R. Gair, Phys. Rev. D **86,** 023502 (2012).

[13] S. R. Taylor, J. R. Gair, and I. Mandel, Phys. Rev. D **85,** 023535 (2012).

[14] B. P. Abbott and R. E. A. Abbott, Rep. Prog. Phys. **72,** 076901 (2009).

[15] P. Amaro-Seoane *et al.*, arXiv:1702.00786.

[16] X. Deng and L. S. Finn, Mon. Not. R. Astron. Soc. **414,** 50 (2011).

[17] A. N. Lommen, J. Phys. Conf. Ser. **363,** 012029 (2012).

[18] L. Z. Kelley, L. Blecha, L. Hernquist, A. Sesana, and S. R. Taylor, Mon. Not. R. Astron. Soc. **477,** 964 (2018).

[19] J. P. W. Verbiest and G. M. Shaifullah, Classical Quant. Grav. **35,** 133001 (2018).

[20] S. Burke-Spolaor, S. R. Taylor, M. Charisi, T. Dolch, J. S. Hazboun, A. M. Holgado, L. Z. Kelley, T. J. W. Lazio, D. R. Madison, N. McMann, C. M. F. Mingarelli, A. Rasskazov, X. Siemens, J. J. Simon, and T. L. Smith, Astron. Astrophys. Rev. **27,** 5 (2019).

[21] X. Siemens, J. Ellis, F. Jenet, and J. D. Romano, Classical Quant. Grav. **30,** 224015 (2013).

[22] S. R. Taylor, M. Vallisneri, J. A. Ellis, C. M. F. Mingarelli, T. J. W. Lazio, and R. van Haasteren, Astrophys. J. Lett. **819,** L6 (2016).

[23] A. Sesana, A. Vecchio, and M. Volonteri, Mon. Not. R. Astron. Soc. **394,** 2255 (2009).

[24] V. Ravi, J. S. B. Wyithe, R. M. Shannon, G. Hobbs, and R. N. Manchester, Mon. Not. R. Astron. Soc. **442,** 56 (2014).

[25] P. A. Rosado, A. Sesana, and J. Gair, Mon. Not. R. Astron. Soc. **451,** 2417 (2015).

[26] D. J. D'Orazio and A. Loeb, Phys. Rev. D **101,** 083031 (2020).

[27] A. Sesana and A. Vecchio, Phys. Rev. D **81,** 104008 (2010).

[28] N. J. Cornish, arXiv:gr-qc/0304020.

[29] K. J. Lee, N. Wex, M. Kramer, B. W. Stappers, C. G. Bassa, G. H. Janssen, R. Karuppusamy, and R. Smits, Mon. Not. R. Astron. Soc. **414,** 3251 (2011).

[30] S. R. Taylor, E. A. Huerta, J. R. Gair, and S. T. McWilliams, Astrophys. J. **817,** 70 (2016).

[31] V. Corbin and N. J. Cornish, arXiv:1008.1782.

[32] R. Angélil and P. Saha, Phys. Rev. D **91,** 124007 (2015).

[33] L. S. Finn and A. N. Lommen, Astrophys. J. **718,** 1400 (2010).

[34] M. Anholm, S. Ballmer, J. D. E. Creighton, L. R. Price, and X. Siemens, Phys. Rev. D **79,** 084030 (2009).

[35] L. G. Book and É. É. Flanagan, Phys. Rev. D **83,** 024024 (2011).

[36] C. McGrath and J. Creighton, arXiv:2011.09561.

[37] J. A. Ellis, Classical Quant. Grav. **30,** 224004 (2013).

[38] R. Smits, S. J. Tingay, N. Wex, M. Kramer, and B. Stappers, Astron. Astrophys. **528,** A108 (2011).

[39] A. T. Deller, J. Boyles, D. R. Lorimer, V. M. Kaspi, M. A. McLaughlin, S. Ransom, I. H. Stairs, and K. Stovall, Astrophys. J. **770,** 145 (2013).

[40] C. M. F. Mingarelli, L. Anderson, M. Bedell, and D. N. Spergel, arXiv:1812.06262.

[41] M. J. Rioja and R. Dodson, Astron. Astrophys. Rev. **28,** 6 (2020).

[42] M. Johnson *et al.*, Bull. Am. Astron. Soc. **51,** 235 (2019), https://ui.adsabs.harvard.edu/abs/2019BAAS...51g.235J.

[43] L. I. Gurvits, arXiv:1810.01230.

[44] A. T. Deller, W. M. Goss, W. F. Brisken, S. Chatterjee, J. M. Cordes, G. H. Janssen, Y. Y. Kovalev, T. J. W. Lazio, L. Petrov, B. W. Stappers, and A. Lyne, Astrophys. J. **875,** 100 (2019).

[45] G. Janssen, G. Hobbs, M. McLaughlin, C. Bassa, A. Deller, M. Kramer, K. Lee, C. Mingarelli, P. Rosado, S. Sanidas, A. Sesana, L. Shao, I. Stairs, B. Stappers, and J. P. W. Verbiest, *Advancing Astrophysics with the Square Kilometre Array (AASKA14)* (2015), https://ui.adsabs.harvard.edu/abs/2015aska.confE..37J.

[46] E. Keane *et al.*, *Advancing Astrophysics with the Square Kilometre Array (AASKA14)* (2015), https://ui.adsabs.harvard.edu/abs/2015aska.confE..40K.

[47] D. R. Lorimer, A. J. Faulkner, A. G. Lyne, R. N. Manchester, M. Kramer, M. A. McLaughlin, G. Hobbs, A. Possenti, I. H. Stairs, F. Camilo, M. Burgay, N. D'Amico, A. Corongiu, and F. Crawford, Mon. Not. R. Astron. Soc. **372,** 777 (2006).

[48] R. Smits, M. Kramer, B. Stappers, D. R. Lorimer, J. Cordes, and A. Faulkner, Astron. Astrophys. **493,** 1161 (2009).

[49] F. Crawford, V. M. Kaspi, R. N. Manchester, A. G. Lyne, F. Camilo, and N. D'Amico, Astrophys. J. **553,** 367 (2001).

[50] R. N. Manchester, G. Fan, A. G. Lyne, V. M. Kaspi, and F. Crawford, Astrophys. J. **649,** 235 (2006).

[51] J. P. Ridley, F. Crawford, D. R. Lorimer, S. R. Bailey, J. H. Madden, R. Anella, and J. Chennamangalam, Mon. Not. R. Astron. Soc. **433,** 138 (2013).

[52] N. Titus, S. Toonen, V. A. McBride, B. W. Stappers, D. A. H. Buckley, and L. Levin, Mon. Not. R. Astron. Soc. **494,** 500 (2020).

[53] S. Chatterjee, in *Science with a Next Generation Very Large Array*, Astronomical Society of the Pacific Conference Series, Vol. 517, edited by E. Murphy (2018), p. 751, https://ui.adsabs.harvard.edu/abs/2018ASPC..517..751C.

[54] R. E. Sanderson, A. Bellini, S. Casertano, J. R. Lu, P. Melchior, M. Libralato, D. Bennett, M. Shao, J. Rhodes, S. T. Sohn, S. Malhotra, S. Gaudi, S. M. Fall, E. Nelan, P. Guhathakurta, J. Anderson, and S. Ho (WFIRST Astrometry Working Group), J. Astron. Telesc. Instrum. Systems **5,** 044005 (2019).

[55] S. Taylor, J. Ellis, and J. Gair, Phys. Rev. D **90,** 104028 (2014).

[56] X. J. Zhu, L. Wen, G. Hobbs, Y. Zhang, Y. Wang, D. R. Madison, R. N. Manchester, M. Kerr, P. A. Rosado, and J. B. Wang, Mon. Not. R. Astron. Soc. **449,** 1650 (2015).